

On the Limitations of Metameric Imaging

Friedhelm König and Patrick G. Herzog
Aachen University of Technology
Technical Electronics Department
Aachen, Germany

Abstract:

Today, color imaging is based on three-channel processing throughout the whole imaging chain including image capture, storage, transmission, and reproduction. This is made possible by the use of metameric colors for color reproduction, hence we call this system metameric imaging.

Unfortunately metamerism bears the potential of errors for each step of the reproduction chain. The aim of this paper is to present the results of an extensive study of the various system errors due to metamerism, and to compare these with a multispectral imaging system which captures spectral information.

The following error sources have been examined:

1. Violation of the Luther-condition
2. Change of illuminant
3. Three-channel-image reproduction

The investigations have shown that there is a large potential for errors in metameric imaging systems. On the other hand, multispectral imaging is able to virtually eliminate these errors.

Introduction

Color is a sensation caused by a stimulus of electromagnetic radiation within the wavelength range from approx. 380 nm to 780 nm [1].

With knowledge of the cone sensitivities of the human eye, the reaction of the cones to the spectral stimulus can be modeled by applying spectral integration to the stimulus. This process results in tristimulus values.

The same color can be described either by the spectral stimulus in form of the n -vector or by the three-dimensional tristimulus vector. The former approach represents the physical realm and is realized by *multispectral imaging*. A stimulus scanned by multispectral imaging does not tell us which color is perceived, but it provides the possibility to compute tristimulus values for arbitrary viewing conditions, if the spectrum of the illuminant is specified additionally.

A disadvantage of the multispectral approach is the large amount of data needed. It has been shown, however, that efficient coding schemes can be found to reduce the amount of necessary data, and that such coding schemes can even be made compatible to conventional imaging [2-3].

The tristimulus approach, on the other hand, uses tristimulus values to represent the scanned color directly, but only for specific viewing conditions. Different stimuli are sometimes mapped to the same tristimulus values. This phenomenon is typical for the tristimulus approach and is called metamerism. Therefore, color imaging based on the processing of tristimulus values is called *metameric imaging* or *three-channel imaging*.

While the metameric approach is sufficient for a wide range of applications, it is not well suited for applications where an exact reproduction is paramount. The archiving and reproduction of fine art paintings are typical examples.

A detailed discussion of the error types introduced by metameric imaging can be found in reference [4]. While the limitations of metameric imaging are generally understood, little knowledge is available about the magnitude of the resulting errors.

The aim of this paper is to give an idea of the size of these errors. Furthermore, the color quality of metameric versus multispectral imaging is discussed.

Spectra, vectors and data sets

For numerical calculations, it is convenient to represent spectra by a number of sample values. Here, the reflectance (or transmittance) spectrum of an object is represented by an n -dimensional vector \mathbf{f} , whose elements are the sample values of the spectrum. The spectral power distribution of the illuminant is written as an $n \times n$ -diagonal matrix \mathbf{L} . The stimulus \mathbf{g} can then be calculated by:

$$\mathbf{g} = \mathbf{L} \mathbf{f}. \quad (1)$$

A p -channel color sensor is represented by a $p \times n$ -matrix \mathbf{M} , the rows of which contain the sensitivities of each channel. Then, the sensor response \mathbf{c} is a p -dimensional vector and can be calculated by:

$$\mathbf{c} = \mathbf{M} \mathbf{L} \mathbf{f}. \quad (2)$$

Within the context of this paper, three different sensor types have been used. These are the human eye, represented by the standard observer (\mathbf{M}_{xyz}), a typical commercial three-channel sensor (Sharp, $\mathbf{M}_{\text{Sharp}}$, see Figure 1) and a 16-channel sensor ($\mathbf{M}_{\text{Multi}}$) which represents multispectral imaging. Such a sensor is used in multispectral scanners to approximate the spectrum of a color. Details on multispectral imaging can be found in [2-9].

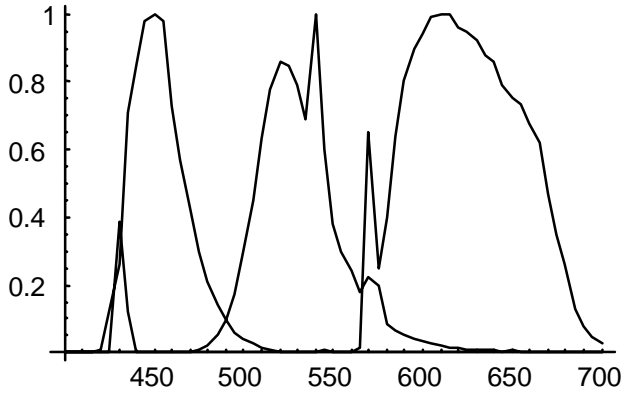


Figure 1. The sensitivities of a Sharp scanner used in the simulations.

In the simulations, two different sets of spectral reflectances were used. The first of these sets (VRHEL) was measured by Vrhel, Gershon and Iwan [10]. It contains 354 spectra of Munsell chips, DuPont chips, and natural objects and was considered to be rather representative of existing spectra.

These spectra were supplemented by a second set (MITSU) which was measured by the authors. It contains the spectra of 234 random color patches printed on a Mitsubishi S 3600-30 thermal sublimation printer. These data were used as an example of conventional three channel technology.

Additionally, a third set, measured by Parkkinen, Hallikainen and Jaaskelainen [11], was evaluated. It was decided, however, not to use this set, because the preliminary results using this set have not been substantially different from those of the VRHEL set.

The illuminants used were A, C, D65, D50, E, F11 and F2.

Limitations of metameric image acquisition

The first step in image reproduction is to acquire the color information of the original image. Typically, a scanner or a CCD-camera is used to this end.

It would be ideal from a color science point of view if the sensitivities of the scanner were the color matching curves of the standard observer or a linear combination thereof. This is called the Luther condition. If this condition is violated, there is an ambiguous relationship between the measured device dependent R, G and B signals and the respective colorimetric values.

Unfortunately, from a technical point of view, there are some serious reasons to choose sensitivities which violate the Luther condition.

Scanning errors due to the violation of the Luther condition are therefore typical for commercial image acquisition devices, although these errors are not unavoidable as a matter of principle. Hence, the question for the magnitude of image acquisition errors cannot be answered ultimately, as the answer is dependent on the image acquisition device used. Nevertheless, it is possible to

give some information about the typical magnitude of errors due to the violation of the Luther condition.

Characterizing scanners

To estimate the magnitude of these errors, a simulation was carried out. We calculated the tristimulus values X, Y and Z and the resulting CIE L^* , a^* and b^* values of all the spectra contained in the VRHEL set.

Likewise, the capture of the same spectra with the Sharp scanner was simulated to calculate the respective scanner output signals R, G and B.

The scanner it must be characterized to evaluate its performance, this means that L^* , a^* and b^* values have to be computed from the scanner outputs R, G and B. We chose a polynomial estimation function:

$$L^*_{estim} = \sum_{i+j+k \leq p} L_{i,j,k} \cdot R^i \cdot G^j \cdot B^k \quad (3)$$

$$a^*_{estim} = \sum_{i+j+k \leq p} a_{i,j,k} \cdot R^i \cdot G^j \cdot B^k$$

$$b^*_{estim} = \sum_{i+j+k \leq p} b_{i,j,k} \cdot R^i \cdot G^j \cdot B^k$$

where p is the polynomial order. The coefficients $L_{i,j,k}$, $a_{i,j,k}$ and $b_{i,j,k}$ are chosen to minimize the ΔE_{ab} color difference.

The polynomial order p has to be chosen carefully, because high order polynomial approaches tend to oscillate. In the simulations, a fourth order polynomial worked best.

Additionally, the multispectral capture of the same spectra was simulated. The smoothing inverse [12] was used as reconstruction algorithm.

The simulation results for both the three-channel scanner and the multispectral scanner can be found in Table 1. The mean errors of the three-channel scanner were about $1.3 \Delta E_{94}$ units with maximum error as high as $7.2 \Delta E_{94}$ units. On the other hand, the multispectral scanner performed almost perfectly, and mean errors as low as $0.01 \Delta E_{94}$ units could be achieved persistently.

Table 1: Mean and maximum scanning errors using random spectra (VRHEL)

illuminant	three-channel scanner		multispectral scanner	
	mean ΔE_{94}	max ΔE	mean ΔE_{94}	max ΔE_{94}
A	1.43	7.22	0.01	0.04
C	1.35	5.45	0.01	0.06
D65	1.33	5.27	0.01	0.06
D50	1.35	5.50	0.01	0.05
E	1.35	5.45	0.01	0.06
F11	1.07	6.48	0.01	0.14
F2	1.24	6.01	0.01	0.04

The simulation did not consider noise or the effects of a limited number of quantization bits. Thus, it is expected that a physical device will perform inferior, and the simulation results for the three-channel scanner can be seen as the

theoretical accuracy limits for the typical spectral characteristics used during the simulation with a fourth order polynomial approach.

Adaptation to the scanned medium

Considerable improvements in the characterization accuracy can be achieved if the variability of the scanned spectra is limited to that of a certain medium. For example, if a scanner is supposed to capture only film material, a match of the characterization to only film material makes sense. As an example for medium adaptation, the characterization of the scanner using the MITSU set was simulated. Then the achieved accuracy was tested using the same data set.

The results can be found in Table 2. The performance of the three-channel scanner improved drastically, and mean errors of about $0.6 \Delta E_{94}$ units could be achieved. The maximum error was below $2.7 \Delta E_{94}$ units for all the cases examined.

It was found that higher order polynomials (polynomial order > 4) showed large oscillations. Hence, the remaining errors of the adapted scanner are mostly the result of instabilities during the printing process and measurement errors during the acquisition of the MITSU set. Due to these errors, the relationship between the scanner's R, G and B signals and the spectral reflectance f is only approximately known. This causes the remaining errors.

The multispectral scanner was used for comparison. It still performed superior by far. The results obtained were similar to those obtained using the VRHEL set.

Table 2: Mean and maximum ΔE_{94} scanning errors with the MITSU data set

illuminant	three-channel scanner		multispectral scanner	
	mean ΔE_{94}	max ΔE_{94}	mean ΔE_{94}	max ΔE_{94}
A	0.61	2.14	0.03	0.06
C	0.60	2.50	0.04	0.09
D65	0.59	2.58	0.04	0.09
D50	0.59	2.39	0.04	0.08
E	0.61	2.41	0.04	0.09
F11	0.61	2.61	0.01	0.04
F2	0.57	2.34	0.03	0.05

Metameric imaging and different illuminants

The illuminant under which an image is reproduced is not necessarily identical to the illuminant used for image acquisition. Often, the reproduction illuminant is not even known prior to printing. In multispectral imaging, the acquisition illuminant is known and can be eliminated by white calibration. Then, the spectral reflectance of the image is available and the color stimulus of a reproduction scenario can be calculated exactly if the illuminant is known. No additional errors are introduced.

If three-channel imaging is used, no information on the spectral reflectance is available. It is not a simple task to

estimate the unknown L^*_{repro} , a^*_{repro} and b^*_{repro} of a colorant viewed under the destination illuminant from the known L^*_{scan} , a^*_{scan} and b^*_{scan} of the same colorant viewed under the illuminant used during image acquisition.

Contrary to the image acquisition problems discussed above, this is one of the fundamental problems of metameric imaging and not caused by technical limits.

To determine the magnitude of the errors caused by the change of the illuminant, colorimetric values were calculated for every spectrum contained in the VRHEL set with both the source and the destination illuminant.

Again, a polynomial estimation function was chosen, and again, a fourth order approach worked best. Table 3 gives the mean and maximum ΔE_{94} errors between the estimated and the exact values for a number of illuminants. Depending on the examined pair of illuminants these errors can be as high as $0.8 \Delta E_{94}$ units (mean) or $6.0 \Delta E_{94}$ units (maximum) respectively.

Not surprisingly, the results indicate that the illuminant during image acquisition should be as close as possible to the reproduction illuminant to minimize errors due to the change of the illuminants. If the reproduction illuminant is not known during the image acquisition, fluorescent tubes should be avoided for image acquisition because of the peaks.

Table 3: Mean (a) and maximum (b) errors in ΔE_{94} caused by the change of the illuminant (VRHEL)

		reproduction illuminant							
		A	C	D65	D50	E	F11	F2	
acquisition illuminant	A	a	0	0.68	0.70	0.50	0.62	0.90	0.64
		b	0	3.45	3.68	2.65	3.08	5.98	3.02
	C	a	0.58	0	0.06	0.17	0.10	0.69	0.44
		b	2.90	0	0.32	2.11	0.42	2.72	2.76
	D65	a	0.60	0.06	0	0.17	0.13	0.68	0.46
		b	3.13	0.32	0	0.89	0.59	2.69	2.76
	D50	a	0.44	0.17	0.18	0	0.14	0.67	0.45
		b	2.04	1.19	0.93	0	0.83	3.05	2.53
	E	a	0.53	0.09	0.13	0.14	0	0.66	0.44
		b	2.70	0.41	0.63	0.78	0	2.64	2.64
	F11	a	0.84	0.84	0.69	0.69	0.67	0	0.52
		b	4.39	2.86	2.97	2.72	2.70	0	4.10
	F2	a	0.71	0.47	0.49	0.49	0.47	0.54	0
		b	3.52	2.57	2.51	2.63	2.67	4.05	0

Analogous with scanner characterization, the illuminant cast can be optimized for the input medium as well. To demonstrate this, the estimation algorithm was adapted to the MITSU set. The results are given in Table 4. The maximum error was below $1 \Delta E_{94}$ unit for all examined cases while the mean error was below $0.2 \Delta E_{94}$ units. The remaining errors once again are mainly caused by inaccuracies within the calibration data.

Table 4: Mean (a) and maximum (b) errors in ΔE_{94} caused by the change of the illuminant (MITSU)

		reproduction illuminant							
		A	C	D65	D50	E	F11	F2	
acquisition illuminant	A	a	0	0.09	0.08	0.05	0.08	0.10	0.10
		b	0	0.32	0.29	0.21	0.28	0.38	0.39
	C	a	0.15	0	0.01	0.04	0.03	0.08	0.07
		b	0.92	0	0.05	0.20	0.14	0.38	0.25
	D65	a	0.14	0.01	0	0.04	0.02	0.08	0.07
		b	0.93	0.05	0	0.22	0.16	0.33	0.26
	D50	a	0.09	0.04	0.03	0	0.02	0.07	0.07
		b	0.56	0.18	0.16	0	0.10	0.28	0.29
	E	a	0.12	0.02	0.02	0.02	0	0.07	0.06
		b	0.75	0.13	0.15	0.10	0	0.32	0.22
	F11	a	0.16	0.09	0.09	0.09	0.08	0	0.08
		b	0.76	0.45	0.43	0.40	0.45	0	0.27
F2	a	0.16	0.06	0.07	0.08	0.06	0.07	0	
	b	0.88	0.23	0.25	0.29	0.24	0.33	0	

Image reproduction - the influence of printer and observer

After an image has been scanned and the image data have been adapted to the reproduction illuminant, the image is printed. In an optimal three-channel system, the print is a metameric match of the original image if it is examined under the reproduction illuminant. However, the reproduction quality is limited for two reasons.

First, the illuminant under which a reproduction is examined is not always known in advance. Furthermore, the reproduction might be viewed under more than one illuminant. For example, the catalogue of a mail-order company is supposed to be viewed under daylight as well as under incandescent light.

Second, the match is only exact for the standard observer. It is known, however, that there are individual differences in the cone responses and moreover, it is suspected, that the standard observer does not perfectly resemble average human sensitivities [13-16].

To examine the magnitude of errors caused by these two limitations, it is necessary to find a model for a typical printer, which allows to calculate the spectral reflectance of a printed color for a given set of tristimulus values. We used the MITSU set to model the Mitsubishi S 3600-30 thermal sublimation printer.

Modeling the printer

First of all, we applied principal component analysis (PCA) to the MITSU set to determine the characteristic eigenvectors \mathbf{e}_i of the set. Next, the eigenvectors \mathbf{e}_i were sorted according to the respective eigenvalues E_i , as described in equation (4):

$$i > j \Rightarrow E_i \geq E_j \quad (4)$$

It is a well known property of PCA, that an eigenvector \mathbf{e}_i belonging to a large eigenvalue E_i is more important to describe the data contained within the data set than a second

eigenvector belonging to a smaller eigenvalue. Therefore a printed spectrum \mathbf{f} can be approximated using the first m of the n eigenvectors:

$$\mathbf{f}_{estim} = \sum_{i=1}^m c_i \cdot \mathbf{e}_i \approx \sum_{i=1}^n c_i \cdot \mathbf{e}_i = \mathbf{f}, \quad (5)$$

where c_i are suitable constants. We used $m = 16$ eigenvectors and the approximation was excellent. The remaining error of each spectral sample value was below 10^{-10} .

The next step was to find functions f_i to calculate the constants c_i from a given set of CIE $L^*a^*b^*$ values as shown in equation (6):

$$c_i = f_i(L^*, a^*, b^*) \quad (6)$$

Again a polynomial approach was chosen. This time, a 6th order approach worked best. By combining equations 5 and 6, we can estimate the spectral reflectances of all printed colors.

This technique was used to generate a metameric match for each spectrum of the VRHEL set under each illuminant. This metameric match was subsequently compared to the original color, seen under a variety of illuminants. The results are shown in Table 5.

Table 5: Mean (a) and maximum (b) ΔE_{94} differences between original and printed colors under a variety of illuminants (VRHEL)

		output examined under illuminant							
		A	C	D65	D50	E	F11	F2	
metameric match under illuminant	A	a	0.02	3.45	3.49	2.59	2.97	2.61	2.68
		b	0.65	11.3	11.0	8.01	8.74	15.4	15.6
	C	a	2.89	0.02	0.16	0.88	0.55	3.16	1.69
		b	6.64	0.79	1.14	2.43	1.30	9.31	5.34
	D65	a	2.86	0.16	0.02	0.84	0.59	3.13	1.71
		b	6.78	1.02	0.72	1.90	1.32	9.10	5.62
	D50	a	2.16	0.89	0.86	0.01	0.54	2.59	1.52
		b	5.98	3.64	3.15	0.64	3.49	6.68	7.14
	E	a	2.53	0.57	0.62	0.51	0.02	2.73	1.49
		b	8.17	2.72	2.45	2.00	0.65	7.06	5.84
	F11	a	2.29	3.17	3.24	2.64	2.75	0.02	1.68
		b	8.15	8.98	8.99	6.91	6.91	0.79	7.42
F2	a	2.67	1.89	1.95	1.59	1.56	1.96	0.02	
	b	12.9	8.04	8.04	7.31	7.25	12.5	0.50	

First, it can be seen that the metameric match is not perfect, otherwise the diagonal of the table should be zero. Nevertheless, the match is reasonably close. A better match would require a more complex printer model.

Apart from this, the results show that there can be considerable color differences of up to $\Delta E_{94} = 16$ between the original and the printed color, if the comparison is not carried out under the reproduction illuminant.

This is a systematic error, which is caused by the use of different color pigments or dyes for the original image and

its copy. The actual size of the error is dependent on the color pigments involved.

For example, if the same experiment was repeated using the MITSU set, there would be almost no difference between the original spectrum and the spectrum used as its metameric match, because the same dyes were used for both images. Unfortunately, this is usually not the case.

The only real solution to avoid the printing problem is multispectral printing, which currently is in a very early stage of development [8].

Non-standard observers

The second problem of metameric color printing is the deviation of an observer from the standard observer. Usually these deviations are quite small, but they might be of interest if anomalous color vision or technical three-channel sensors are considered.

Several authors report that even normal color vision is based on clearly different spectral cone responses [13-15]. Therefore, deviations from the standard observer have to be considered.

Keusen [5] simulates anomalous color vision by modifying the spectral sensitivity $l(\lambda)$, $m(\lambda)$ and $s(\lambda)$ of the cones of the human eye. A generic observer is described by equations 7:

$$l'(\lambda) = k_l l(\lambda - \Delta\lambda_l) \quad (7)$$

$$m'(\lambda) = k_m d(\lambda - \Delta\lambda_m)$$

$$s'(\lambda) = k_s t(\lambda - \Delta\lambda_s)$$

The constants $\Delta\lambda_l$, $\Delta\lambda_m$ and $\Delta\lambda_s$ describe a wavelength shift of the spectral sensitivity curves of the respective cones. The constants k_l , k_m and k_s allow to reduce the sensitivity of the respective cones.

The standard observer exhibits neither a wavelength shift ($\Delta\lambda_l = \Delta\lambda_m = \Delta\lambda_s = 0$ nm) nor a reduced sensitivity ($k_l = k_m = k_s = 1$).

Of the different types of non-standard observers described by Keusen, two types are especially interesting in the context of this paper. They differ from the standard observer by a shift of the sensitivity of the l-cones towards lower wavelengths by $\Delta\lambda_l = 1$ nm or $\Delta\lambda_l = 5$ nm respectively. Otherwise these observers are identical to the standard observer.

Table 6: Color differences in ΔE_{94} for a non-standard observer between a color and its metameric match

illuminant	$\Delta\lambda_l = 1$ nm		$\Delta\lambda_l = 5$ nm	
	mean	max	mean	max
A	0.86	1.49	4.10	6.30
C	0.49	1.62	2.56	8.63
D65	0.49	1.69	2.60	8.93
D50	0.49	1.49	2.57	8.18
E	0.49	1.48	2.57	7.96
F11	0.39	0.94	1.85	5.38
F2	0.34	1.05	1.73	6.04

Both non-standard observers were used to compare the colors of the VRHEL set and their metameric matches. The results can be found in Table 6. While the errors were quite small for the non-standard observer with 1 nm shift (maximum error below $2 \Delta E_{94}$ units), a 5nm shift led to mean errors as high as $4 \Delta E_{94}$ units with maximum errors of about $9 \Delta E_{94}$ units.

These errors can be avoided only if multispectral printing is used in addition to multispectral image acquisition.

Conclusions

In this paper, the limitations of the different stages of metameric imaging were illustrated. A summation of the results can be found in figure 2.

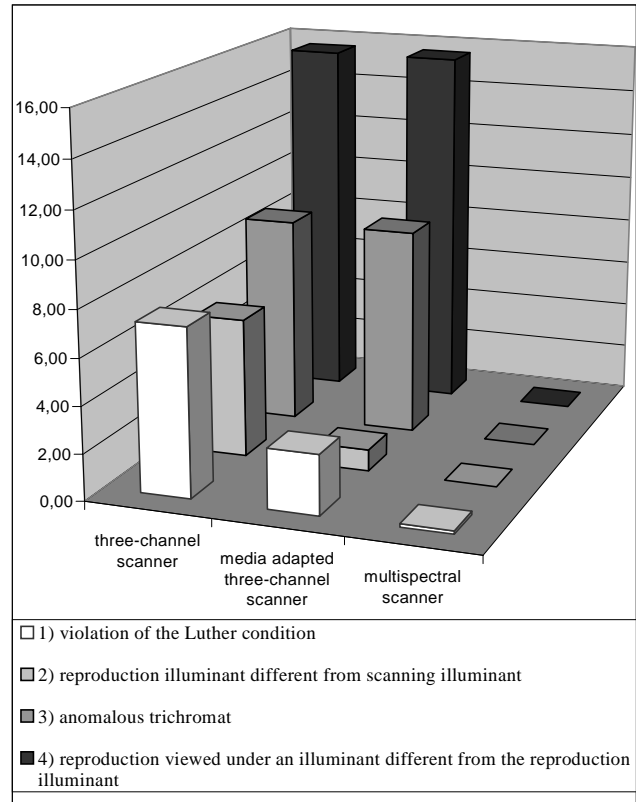


Figure 2. Comparison of the maximum ΔE_{94} errors due to the limitations of metameric three-channel imaging and the maximum errors of multispectral imaging.

With the image acquisition stage, we encountered errors due to the violation of the Luther condition. The size of these errors are dependent on the scanner. A typical commercial scanner produced errors of up to $7 \Delta E_{94}$ units.

Frequently, these errors can be reduced if the original image belongs to a certain media type (e.g. film material), so that the scanner characterization can be adapted to this medium.

Using an adapted scanner, we encountered maximum errors of about $2.5 \Delta E_{94}$ units. A further reduction of the

errors is possible if multispectral imaging is used. Here, maximum errors below $0.2 \Delta E_{94}$ units can be achieved.

If the scanned image has to be adapted to an illuminant different from the scanning illuminant, errors of up to $6.0 \Delta E_{94}$ units were encountered. These errors can be completely avoided by using multispectral imaging.

The largest errors were produced by metameric printing if either the observer is an anomalous trichromat (up to $9 \Delta E_{94}$) or an illuminant different from the reproduction illuminant is chosen (up to $16 \Delta E_{94}$). These errors could be reduced by multispectral printing.

Moreover, it is known that even an average person with normal color vision is not very well represented by the standard observer (CIE 1931) [16]. Furthermore an observer's sensitivities are dependent on the subtended viewing angle, under which a color is examined. These limitations cause additional errors, which cannot be described using the three-channel model. The size of these errors is unknown. Still, it is reasonable to assume these errors to be small, given the success of the widely used three-channel model.

Acknowledgements

This work was supported by the Deutsche Forschungsgemeinschaft (DFG) of Germany. Furthermore, the authors wish to thank Ms. Armelle Kerbaol for her support during the preparation of this paper.

References

1. H. J. Trussell, Applications of Set Theoretic Methods to Color Systems, *Color Res. and Appl.* **16**, 1, 31-41, (1991)
2. F. König and W. Praefcke, A multispectral scanner, *Proc. of CIM'98 Colour Imaging in Multimedia*, 63-73 Derby, UK (1998)
3. T. Keusen, Multispektrale Farbanalyse, Shaker, Aachen, Germany, 1996
4. B. Hill, Multispectral color technology: a way toward high-definition color scanning and encoding, *Proc. of Electronic Imaging: Processing, Printing, and Publishing in Color*, 2-13, Zürich, Switzerland (1998)
5. F. König and W. Praefcke, Practice of multispectral image acquisition, *Proc. of Electronic Imaging: Processing, Printing, and Publishing in Color*, 34-41, Zurich, Switzerland (1998)
6. T. Roger, Multispektrale Farbbildabtastung, eine Möglichkeit zur Gewinnung von vorlagen- und geräteunabhängiger Farbinformation, *Proc. of 9. Aachener Kolloquium „Signaltheorie“ Bild und Sprachsignale*, Aachen, Germany (1997)
7. J. Y. Hardeberg, F. Schmitt, H. Brettel, J-P. Crettez and H. Maître, Multispectral imaging in multimedia, *Proc. of CIM'98 Colour Imaging in Multimedia*, 75-86 Derby, UK (1998)
8. R. S. Berns, Challenges for color science in multimedia, *Proc. of CIM'98 Colour Imaging in Multimedia*, 123-133 Derby, UK (1998)
9. P. D. Burns, Analysis of image noise in multispectral color acquisition, Dissertation at the Rochester Institute of Technology, Rochester, NY, USA, 1997
10. M. J. Vrhel, R. Gershon and L. S. Iwan, Measurement and analysis of object reflectance spectra, *Color Res. and Appl.* **19**, 4, 4-9, (Feb. 1994)
11. J. P. S. Parkkinen, J. Hallikainen and T. Jaaskelainen, Characteristic Spectra of Munsell Colors, *J. Opt. Soc. Am.*, **6**, 2, 318-322, (Feb. 1989)
12. C. E. Mancill, Digital color image restoration, Dissertation at the University of Southern California, Los Angeles, CA, USA, 1975
13. M. Neitz, J. Neitz and G. H. Jacobs, Spectral tuning of pigments underlying red-green color vision, *Science*, **252**, 971-974, (May 1991)
14. S. L. Merbs and J. Nathans, Absorption spectra of the hybrid pigments responsible for anomalous color vision, *Nature*, **356** (2), 433-435, (April 1992)
15. A. J. Williams, D. M. Hunt, J. K. Bowmaker and J. D. Mollon, The polymorphic photopigments of the marmoset: spectral tuning and genetic basis, *The EMBO Journal*, **232**, 2039-2045, (April 1986)
16. W. A. Thornton, Toward a more accurate and extensible colorimetry, Part I – III, *Color Res. & Appl.*, **17**, 79-122, 162-186, 240-262, (1992)